Numerical and experimental study on shear coaxial injectors with hot hydrogen-rich gas/oxygen-rich gas and GH_2/GO_2*

Jin Ping(金 平), Li Mao(李 茂)†, and Cai Guo-Biao(蔡国飙)

Beijing University of Aeronautics and Astronautics, Beijing 100191, *China*

(Received 4 June 2012; revised manuscript received 15 October 2012)

The influences of the shear coaxial injector parameters on the combustion performance and the heat load of a combustor are studied numerically and experimentally. The injector parameters, including the ratio of the oxidizer pressure drop to the combustor pressure (D_P), the velocity ratio of fuel to oxidizer (R_V), the thickness (W_O), and the recess (H_O) of the oxidizer injector post tip, the temperature of the hydrogen-rich gas (T_H) and the oxygen-rich gas (T_O), are integrated by the orthogonal experimental design method to investigate the performance of the shear coaxial injector. The gaseous hydrogen/oxygen at ambient temperature (GH_2/GO_2), and the hot hydrogen-rich gas/oxygen-rich gas are used here. The length of the combustion (L_C), the average temperatures of the combustor wall (T_W), and the faceplate (T_F) are selected as the indicators. The tendencies of the influences of injector parameters on the combustion performance and the heat load of the combustor for the GH_2/GO_2 case are similar to those in the hot propellants case. However, the combustion performance in the hot propellant case is better than that in the GH_2/GO_2 case, and the heat load of the combustor is also larger than that in the latter case.

Keywords: gas–gas injector, combustion performance, heat load, experiment

PACS: 47.70.Pq, 47.54.De, 44.05.+e **DOI:** 10.1088/1674-1056/22/4/044701

1. Introduction

With the development of astronautics technology over the past several decades, the reusable launch vehicle has gained substantial attention due to its low launch cost and high reliability.[1] The full flow stage cycle (FFSC) engine has been selected as one of the next-generation reusable launch vehicles due to its high performance and reliability.[2] The gas–gas injector has been identified as a key technique for the FFSC engine.[3,4] Many research results of the gas–gas injector have been obtained through considerable numerical simulations, experiments, and optimal designs by designers in the rocket engine field. Among this research, many advanced techniques, such as the optical measurement and the large eddy simulation (LES), are widely used.[5–12]

In order to explore the approach to the optimal design of the injector, Shyy *et al.*[13] used different optimization methods to study the gas–gas injector. In their work, the propellant mixture ratio, the velocity ratio of fuel to oxidizer, and the combustor length (the length from the injector to the throat) were selected as the design parameters; the optimal energy release efficiency, and the heat flux were selected as the objectives. Vaidyanathan *et al.*[14] employed a computational fluid dynamics (CFD) method to study the single-objective and the multi-objective optimization for the coaxial injector. They conducted an in-depth analysis of the influence of the injector design parameters on the performance and the lifetime of the engine. Coley *et al.*[15] used hydrogen/oxygen at ambient temperature (GH_2/GO_2) to investigate the influences of the pressure and the combustor length on the wall heat flux and the injector face temperature in a single element shear injector. Relevant studies have been focused on the gas–gas injector that uses the GH_2/GO_2 as the propellants.

Marshall *et al.*[16] used both the hot hydrogen-rich gas/oxygen-rich gas provided by the preburners and the GH_2/GO_2 to study a gas–gas injector. They found that the maximum heat flux level is about twice that in the hot propellant case. Benchmark quality data were provided for the CFD code through their effort.[17] To improve the credibility of the numerical approach, the hot propellants were used as the boundary conditions in simulations by Tucker *et al.*[18] and Sozer *et al.*[19]

Compared with the experimental system of a combustor using the GH_2/GO_2, the one using hot propellants is much more complex and expensive. This is because of the design requirement of installing an oxidizer-rich preburner (which is another key technique for the FFSC engine), the fuel preburner, and the corresponding igniters. If the results obtained from the GH_2/GO_2 case could be used to predict the laws of the hot propellants, both the cost and the difficulty of the experiment will be reduced effectively, which would lead to a significant development on the gas–gas combustion.

The shear coaxial injector is selected in the present work. The parameters are integrated by the orthogonal experimental design method, and the combustion flowfield is simulated.

*Project supported by the National High Technology Research and Development Program of China (Grant No. 2009702504).

†Corresponding author. E-mail: limaobuaa@hotmail.com

© 2013 Chinese Physical Society and IOP Publishing Ltd

The influences of injector parameters on the combustion performance and the heat load of the combustor are studied numerically and experimentally, and the relationship and the difference between the GH_2/GO_2 case and the hot propellants case are obtained.

2. Numerical model and methods

2.1. Injector and combustor model

Based on the style of the injection, there are various types of injectors usually used in the liquid rocket engine, including the centrifugal, the impinging, and the shear. The centrifugal injector can improve the mixing process of the propellants through circumrotation. The impinging injector can promote the mixing process by the head-on interaction between the oxidizer and the fuel. The shear injector can accomplish the mixing process through the shear-mixing of the propellants. Generally, the first two types have a better mixing effect, thus leading to a higher combustion performance than the last type. However, the combustion zones in the first two types of injectors are closer to the faceplates of the injectors, leading to a higher temperature of the injectors and consequently serious conditions for the thermal protection. As a result, the shear coaxial injector is selected here. A single element combustor of the circular cross section with a diameter of 26 mm and a total length of 290 mm is used in the study as shown in Fig. 1. The overall mass flow mixture ratio (R_C) is 6.0, and the total mass flow ($\dot{m}_C$) is nominally 226 g/s at the design combustor pressure of 3.0 MPa.

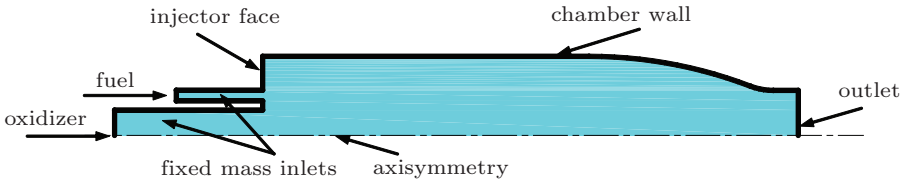


Fig. 1. Model of the combustor and injector.

2.2. Numerical method and boundary conditions

The accuracy of the simulation model is always the issue that concerns injector designers most. In recent years, a lot of techniques in computational fluid dynamics (CFD) have been developed. To satisfy the needs of providing new design tools for the injector, different CFD codes (particularly the large eddy simulation (LES) approaches) have been studied by researchers. Tucker *et al*.[18] used five different CFD codes, i.e., three different LES approaches, the unsteady Reynolds–Averaged Navier–Stokes approach (URANS), and the steady Reynolds–Averaged Navier–Stokes (RANS) approach, to compute the combustion flowfield for a single element combustor. One of the LES results showed very good agreement with the experimental data. However, the number of grid points used in that simulation was very large. Additionally, they also found that all of the results matched the experimental data very well over the discrete portions of the chamber wall. Their studies aimed at improving the credibility of simulations.

Although some LES approaches indeed provide good results for design, the requirements of a large mesh size and a long computing time make them impossible for engineering applications now. The low computational cost and the high computational efficiency are the characteristics of the RANS approach. Sozer *et al*.[19] summarized and listed some simulation methods for the gas–gas combustion flowfield. After comparative studies, they considered that the RANS approach can provide comparable results to those by using the LES approach. On the other hand, the RANS approach is widely applied to the injector design. Conley *et al*.[15] used the CFD results based on the RANS approach to conduct an optimal design. Betti *et al*.[20] computed the heat flux of oxygen/methane chambers also with the RANS approach. The numerical results showed that they are in good agreement with the experimental data, except those in the region near the injection. Wang *et al*.[21] have studied different RANS models for the gas–gas combustion flowfield and found a model from which the results obtained are in good agreement with the experimental results. Moreover, they[22–24] have proved the similarity of the gas–gas combustion flowfield to the results obtained from the RANS approach and the experiments. The characteristics of the gas–gas combustion flowfield were studied by Gao *et al*.[25] The high-speed photography instrument was used in their experiments, and the simulation results obtained by RANS well-matches the experimental results.

On the whole, those investigations indicate that the RANS approach can be used to study the gas–gas injector. Especially in comprehensive studies, it can obtain comprehensive information with a low cost in calculation by the RANS. Because of the above reasons, the RANS approach is generally adopted

in practical application. The Navier–Stokes equations, the k–ε turbulence model, and the kinetic equations are to be solved to simulate the combustion flowfield of the combustor in this study, and the steady state is also assumed. The chemical species continuity equations, including a six-species and nine-reaction set, are employed to represent the reaction mechanism with the aid of a six-species.[21,22] Convective terms represente the second-order flux split upwind differential equation, while the diffusion terms are central difference. The oxidizer inlet and the fuel inlet are set be the condition for mass inlet separately. The exit of the nozzle is used as the pressure outlet while all the walls satisfy the no-slip adiabatic wall boundary condition. The axisymmetric boundary condition is set for the axis.

2.3. Parameters of injectors and test battery approach

There is a large range of parameter types involved in the injector design, such as structural variables, pneumatic parameters, etc. Hence, a comprehensive study on all the design parameters can lead to a high computation cost and a very low efficiency. In order to obtain comprehensive and valuable information as much as possible at the lowest computation cost, it is significant to arrange the simulation cases with different parameters. The efficient orthogonal experiment design method is used in this paper. This method is used widely in the field of optimal design.

Both the GH_2/GO_2 and the hot hydrogen-rich gas/oxygen rich gases are used to study the relationships and the differences on the combustion performance and the heat load of the combustor in this work. The hot hydrogen-rich gas and oxygen rich gas are provided by the GH_2/GO_2 hydrogen-rich preburner and the GH_2/GO_2 oxygen-rich preburner, respectively. The injector parameters, including the ratio of the oxidizer pressure drop to the combustor pressure (D_P), the velocity ratio of fuel to oxidizer (R_V), the thickness and the recess of the oxidizer injector post tip (W_O and H_O), the temperatures of the hydrogen-rich gas and the oxygen-rich gas (T_H and T_O), are integrated by the orthogonal experimental design method. The level of each injector design parameter is 5 as shown in Table 1, where R_H and R_O are the mixture ratios of the preburners for the hydrogen-rich gas and the oxygen-rich gas, respectively. The $L_{25}(5^6)$ orthogonal table is used to arrange the parameters. In addition, 25 cases are studied in each case.

Table 1. Values of injector design parameters.

Level	D_P/%	R_V	W_O/mm	H_O/mm	$T_O(R_O)$/K	$T_H(R_H)$/K
1	2	4	0.5	0	577(450)	707(0.40)
2	4	5	1.0	2	622(380)	758(0.45)
3	6	6	1.5	4	676(320)	810(0.50)
4	8	7	2.0	6	724(280)	860(0.55)
5	10	8	2.5	8	777(240)	909(0.60)

In the GH_2/GO_2 case, the mass flow rates of the oxygen and the hydrogen are 193.7 g/s and 32.3 g/s, respectively. In the hot propellant cases, the rate of total mass flow of the oxygen in both preburners is 193.7 g/s, while that of the hydrogen is 32.3 g/s. The mass flow rates of the oxygen and the hydrogen in each preburner are computed through the mixture ratio of preburners and total mass flow rate. They are given by

$$\begin{aligned}
&\dot{m}_{OO} + \dot{m}_{OH} + \dot{m}_{HO} + \dot{m}_{HH} = \dot{m}_C,\\
&(\dot{m}_{OO} + \dot{m}_{HO})/(\dot{m}_{OH} + \dot{m}_{HH}) = R_C,\\
&\dot{m}_{OO}/\dot{m}_{OH} = R_O,\\
&\dot{m}_{HO}/\dot{m}_{HH} = R_H,
\end{aligned}$$

where $\dot{m}_{OO}$ and $\dot{m}_{HO}$ are the mass flow rates of the oxygen, while $\dot{m}_{OH}$ and $\dot{m}_{HH}$ are the mass flow rates of the hydrogen in the oxygen-rich preburner and hydrogen-rich preburner, respectively.

2.4. Evaluation objective

The propellant combustion performance and the heat load of the combustor are two significant parameters used to evaluate the characteristics of an injector. The highest energy release efficiency and the lowest heat load in the combustor, which are essential for the system performance and lifetime, are the goal that is pursued by a rocket motor designer. Unfortunately, the improvement of the combustion performance often leads to increases of the temperatures on the solid surfaces of the injector and the combustor. Therefore, these two parameters are explored in the present work so as to help the injector designer balance the injector performance and the service life. The combustion length (L_C) is selected as the indicator for the combustion performance. L_C is the distance from the injector face to the centerline axial location where the combustion is 90% completed. A short combustion length indicates that the combustion can be completed in a short combustor, which is equivalent to reducing the length and the weight of a combustor. The average gas temperature on the faceplate (T_F) and the average gas temperature on the combustor wall (T_W) are selected as the indirect indicators of the heat load. The injector face is the area from the injector outer diameter to the combustor inner diameter, and the combustor wall is the area of the cylinder inner wall surface without counting the area of the nozzle inner wall surface. In Vaidyanathan *et al.*'s work,[14] the maximum injector face temperature and the wall temperature at a distance three inches away from the injector face (i.e. the gas temperature on the wall) are chosen as the indicators for the evaluating the heat load. In this case, the region under the severest condition is revealed, however it cannot show the heat load of the whole system, which will influence the combustion performance and the cooling system design. As a

result, the average temperature is used to indicate the heat load in this work.

3. Results and discussion

3.1. Analysis of typical results

The injector design parameters are shown in Table 2, where $\dot{m}_O$ and $\dot{m}_H$ are the mass flow rates of the oxidizer and the fuel, respectively. In the hot propellant case, GH_2 and GO_2 are redistributed in preburners, and the mass flow rate of oxygen-rich gas is smaller than that of GO_2 in the GH_2/GO_2 case, while the mass flow rate of hydrogen-rich gas is larger than that of GH_2 in the GH_2/GO_2 case. As a result, the momentum ratio of fuel to oxidizer in the hot propellant case is higher than that in the GH_2/GO_2 case.

Table 2. Values of injector design parameters.

	D_P/%	R_V	W_O/mm	H_O/mm	T_O/K	T_H/K	$\dot{m}_O$/(g/s)	$\dot{m}_H$/(g/s)
GH_2/GO_2	6.5	6.6	1.5	0	300	300	193.7	32.3
Hot propellants	6.5	6.6	1.5	0	676(320)	758(0.45)	180	46

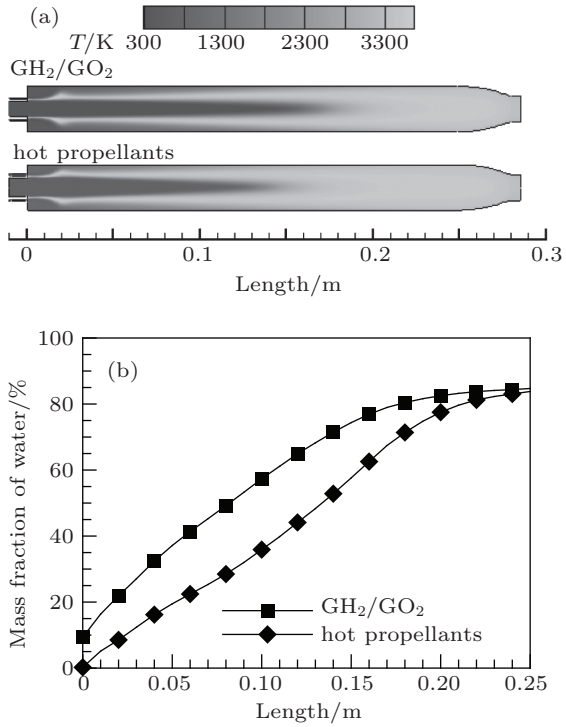


Fig. 2. Distributions of temperature and mass fraction of water in the hot propellant case and GH_2/GO_2 case: (a) temperature, (b) mass fraction of water.

Figure 2 shows the temperature contours in the combustor and the water mass fractions on cross sections for both propellants cases. In the hot propellant case, the high temperature region is closer to the faceplate than in the GH_2/GO_2 case, and the water mass fraction can reach the equilibrium in a relatively short chamber length, which proves that the combustion performance is better. The hydrogen-rich/oxygen-rich gases contain water, so the water mass fraction at the chamber entrance is not zero. Figure 2(b) shows that the water mass fraction in the hot propellant case increases faster, which implies a larger reaction rate. Firstly, a high gas temperature can improve the combustion reaction. Secondly, the momentum ratio of fuel to oxidizer in the hot propellant case is higher than in the GH_2/GO_2 case, which improves the combustion performance. Thirdly, the volume flow rate of hydrogen-rich/oxygen-rich gases is large, which results in a large injector size and a large propellant contact area, so that the combustion is enhanced.

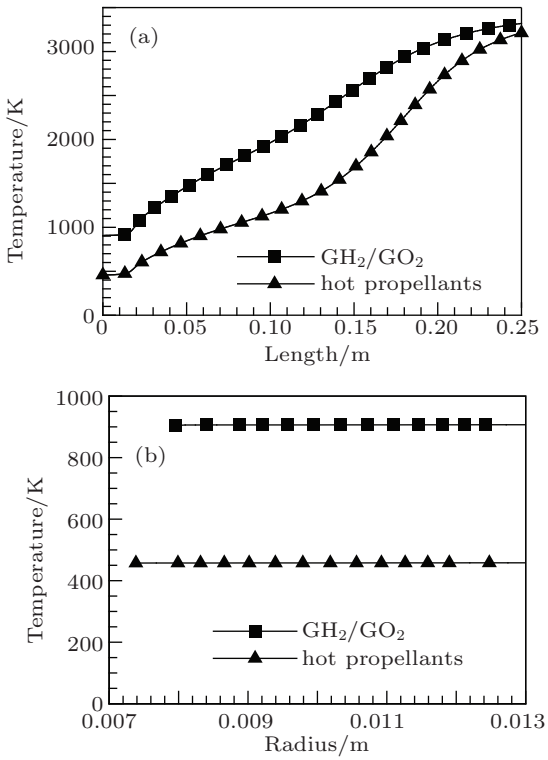


Fig. 3. Temperature distributions in the hot propellant case and GH_2/GO_2 case: (a) combustor wall, (b) faceplate.

Figure 3 gives the gas temperature distributions on the cylinder chamber wall and the faceplate in both cases, and they show that at the same position the temperature in the hot propellant case is higher than that in the GH_2/GO_2 case. With the design parameters in this study, at a place 200 mm away from the faceplate, the gas temperature on the chamber wall in the hot propellant case is about 600 K higher than that in the GH_2/GO_2 case. The maximum value is greater than 1000 K. And the gas temperature on the faceplate is about

450 K greater than in the GH_2/GO_2 case (the propellants flow rate and the temperature in the GH_2/GO_2 case are different from those in the hot propellants case, which results in different outer injector diameters and faceplate sizes). The reasons why the gas temperature in the hot propellant case is obviously higher than that in the GH_2/GO_2 case is as follows. Firstly, in the hot propellant case, propellants at the entrance are at a high temperature, a high temperature gas exists around the faceplate and the front chamber wall, while mainly ambient temperature hydrogen exists around there in the GH_2/GO_2 condition. Secondly, the combustion performance is good and the temperature at the same axial position is relatively high in the hot propellant case. So is the gas temperature on the chamber wall. When the combustion is about to be completed in both cases, the temperature difference decreases. As shown in the figure below, at the position of 250 mm, the gas temperatures on the wall in both cases are similar.

Table 3 gives the values of combustion length, maximum, and the average gas temperature on the chamber wall and the faceplate in the GH_2/GO_2 and the hot propellant case. It shows that the combustion length in the hot propellant case is about 38-mm shorter than that in the GH_2/GO_2 case, and the relative reduction is about 20%. The average gas temperatures on the chamber wall and the faceplate in the hot propellant case are apparently higher than those in the GH_2/GO_2 case. The differences are about 610 K and 450 K, and the relative increases are 42.3% and 98%, respectively. The results prove that the chamber heat load apparently increases if the hydrogen-rich/oxygen-rich gas is used.

Table 3. Values of L_C and T_W in the hot propellants case and GH_2/GO_2 case.

Case	L_C/mm	T_W/K	T_F/K
GH_2/GO_2	197.4	1457.2	458.0
Hot propellants	159.2	2073.8	906.4

3.2. Simulation results and discussion

The parameters and simulation results are shown in Table 4. The temperatures of the propellants in the GH_2/GO_2 case are at 300 K. It can be seen that the combustion lengths are short, and the gas temperatures on the faceplate and the combustor wall are relatively high in the hot propellants case.

Table 4. Parameter setting and simulation results.

Case	D_P/%	R_V	W_O/mm	H_O/mm	T_O/K	T_H/K	GH_2/GO_2			Hot propellants		
							L_C/mm	T_F/K	T_W/K	L_C /mm	T_F/K	T_W/K
case 1	2	4	1.0	6	676	758	210.8	306	1025	193.4	758	1551
case 2	4	4	2.5	8	777	860	216.8	345	1051	187.0	865	1703
case 3	6	4	2.0	0	724	708	236.6	363	970	214.9	749	1512
case 4	8	4	0.5	4	577	810	267.8	415	928	231.6	863	1528
case 5	10	4	1.5	2	622	909	267.6	411	916	222.5	960	1653
case 6	2	5	1.5	4	724	860	195.2	316	1171	170.2	859	1753
case 7	4	5	1.0	2	577	708	209.5	358	1151	184.1	731	1642
case 8	6	5	2.5	6	622	810	211.5	418	1204	177.3	868	1816
case 9	8	5	2.0	8	676	909	225.3	470	1196	178.0	1027	1951
case 10	10	5	0.5	0	777	758	262.9	455	1018	224.0	961	1736
case 11	2	6	0.5	8	622	708	195.7	356	1254	172.5	725	1727
case 12	4	6	1.5	0	676	810	195.3	380	1282	163.7	848	1887
case 13	6	6	1.0	4	777	909	210	457	1285	162.4	1046	2057
case 14	8	6	2.5	2	724	758	211.4	479	1293	173.7	950	1943
case 15	10	6	2.0	6	577	860	216.9	533	1328	169.2	1061	2041
case 16	2	7	2.0	2	777	810	177.8	347	1373	150.2	816	1954
case 17	4	7	0.5	6	724	909	200.4	468	1369	155.5	1037	2092
case 18	6	7	1.5	8	577	758	194.3	540	1474	158.5	975	2041
case 19	8	7	1.0	0	622	860	205.5	500	1370	157.7	1054	2097
case 20	10	7	2.5	4	676	708	201.5	565	1452	160.5	1030	2089
case 21	2	8	2.5	0	577	909	172.1	348	1443	143.0	909	2025
case 22	4	8	2.0	4	622	758	174.6	461	1534	141.9	884	2094
case 23	6	8	0.5	2	676	860	196.8	523	1454	149.1	1095	2179
case 24	8	8	1.5	6	777	708	187.9	609	1590	144.8	1132	2245
case 25	10	8	1.0	8	724	810	212.7	712	1569	151.2	1350	2342

3.2.1. Range analysis of L_C

The simulation results are obtained by using the range analysis method. The results of the range analysis on the combustion length are shown in Tables 5 and 6. The tables show the average values of L_C at the same design parameter and the same level in different cases. For example, the value of average L_C when $D_P = 2\%$ (level 1) is the average value in cases 1,

6, 11, 16, 21. The range in the table is the difference between the maximal value and the minimal value on the condition that the design parameters are the same. A large range means a remarkable influence, *vice versa*.

Table 5. Range analysis results of design parameters on the L_C for the GH_2/GO_2 case.

Parameters	Average of L_C/mm					Range
	Level 1	Level 2	Level 3	Level 4	Level 5	
D_P	190.3	199.3	209.8	219.6	232.3	42.0
R_V	239.9	220.9	205.9	195.9	188.8	51.1
W_O	224.7	209.7	208.0	206.2	202.6	22.1
H_O	214.5	212.6	209.8	205.5	209.0	9.0

Table 6. Range analysis results of design parameters on the L_C for the hot propellant case.

Parameters	Average of L_C/mm					Range
	Level 1	Level 2	Level 3	Level 4	Level 5	
D_P	165.8	166.4	172.5	177.2	185.5	19.6
R_V	209.9	186.7	168.3	156.5	146.0	63.9
W_O	186.5	169.8	171.9	170.8	168.3	18.2
H_O	180.6	175.9	173.3	168.0	169.4	12.6
T_O	177.3	174.4	168.9	173.1	173.7	8.3
T_H	175.4	178.3	174.8	166.7	172.3	11.6

From the results of the range analysis we can conclude that according to the influence degree, the sequence of the injector parameters from large to small in the GH_2/GO_2 case is: R_V, D_P, W_O, H_O. Similarly, the sequence in the hot propellants case is: R_V, D_P, W_O, H_O, T_H, T_O. A comparison between the two propellant cases shows that their sequences are the same if the temperatures of the hydrogen-rich gas and the oxygen-rich gas are neglected. The main characteristics are as follows.

(i) The mixing depends on the shear effect in the shear coaxial injector. And it is influenced significantly by the momentum ratio of fuel to oxidizer. The momentum ratio is equivalent to the velocity ratio in this study, the mixing and the combustion performances therefore are better with a larger velocity ratio.

(ii) The injection velocity of the oxidizer increases with the oxidizer pressure drop ratio increasing. However, the combustion performance cannot be improved a lot because the velocity ratio does not change. Increasing the injection velocity is equivalent to lengthening the mixing length, thus increasing the combustion length.

(iii) The flow characteristics are almost the same in different thicknesses of the oxidizer post tip, and the combustion lengths are almost the same as well.

(iv) Without the atomization and the evaporation in the gas–gas combustion process, the flow and the combustion characteristic are not affected by the recess. The combustion lengths are almost the same in different recess cases.

(v) In the hot propellants cases, the influences of the change of T_H and T_O on the combustion performance are small. The activation energy of the chemical reaction can be lowered and the reaction time can be shortened if the temperature is increased. Compared with the mixing time, however, the chemical reaction time can be ignored. Besides, on the conditions of the same injection velocities and the velocity ratios, the flow characteristics are almost the same for different initial temperatures of the propellants. Moreover, the volume flow rate is relatively large in the hot propellants case. The sizes of the injector and the injection area are large, too, which leads to a large contact area between the fuel and oxidizer, thereby facilitating the mixing and the combustion. The layers of the fuel and the oxidizer are thick so that the mixing length will be lengthened. Combining all the actions, the propellant temperature has only a slight influence on the combustion performance.

Comparing the combustion lengths with the same injector design parameters and the same design levels in both propellants case, it can be seen that the length in the hot propellant case is about 50 mm less than that in the GH_2/GO_2 case. As a result, the combustion performance is relatively good.

The influence tendencies of the design parameters on the average of L_C are shown in Fig. 4. It can be seen that the influence tendencies are similar in the two cases. From the above analysis it follows that the mixing depends on the shear effect in the shear coaxial injector, and the initial temperature of the propellants only has little influence on the mixing. Therefore, the initial temperature is high in the hot propellant case, and the influence law of the design parameters such as the oxidizer pressure drop and the velocity ratio, however, should be the same in different temperature propellant cases. In other words, the influence regularities of the design parameters on the combustion length are the same between the two propellant cases

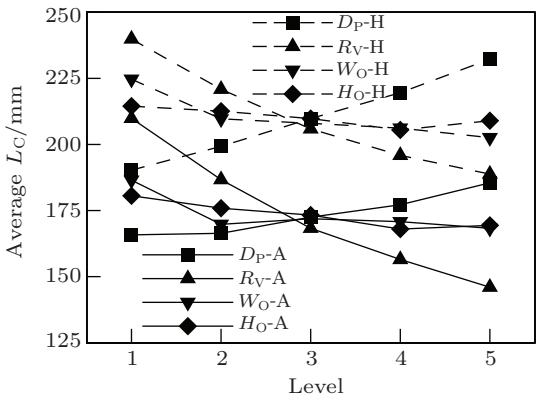


Fig. 4. Effect trends of design parameters on L_C in the hot propellants case and GH_2/GO_2 case.

3.2.2. Range analysis of T_W

The range analyses on the average gas temperature on the combustor wall for the GH_2/GO_2 case and the hot propellant case are shown in Tables 7 and 8, respectively. According to the influence degree, the sequence of the injector parameters from large to small in GH_2/GO_2 case is R_V, D_P, W_O, H_O; while the sequence in the hot propellant case is R_V, D_P, T_H, H_O, W_O, T_O. The reasons are as fellows.

Table 7. Range analysis results of design parameters on the T_W for the GH_2/GO_2 case.

Parameters	Average of T_W/K					Range
	Level 1	Level 2	Level 3	Level 4	Level 5	
D_P	1253	1277	1277	1275	1257	24
R_V	978	1148	1288	1408	1518	540
W_O	1205	1280	1287	1280	1287	84
H_O	1217	1237	1274	1303	1309	92

Table 8. Range analysis results of design parameters on the T_W for the hot propellants case.

Parameters	Average of T_W /K					Range
	Level 1	Level 2	Level 3	Level 4	Level 5	
D_P	1802	1884	1921	1953	1972	170
R_V	1589	1780	1931	2055	2177	588
W_O	1852	1938	1916	1910	1915	86
H_O	1851	1874	1904	1949	1953	101
T_O	1855	1877	1931	1928	1939	84
T_H	1843	1873	1905	1955	1956	113

i) In both propellant cases, the velocity ratio has the largest effect on the results, which means that it is the major factor. From the analysis of the combustion performance, it follows that a large velocity ratio can lead to a good combustion performance, and the combustion can be completed in a short combustor length. Most of the combustor walls are exposed to the high temperature gas, thus causing a high average temperature of the combustor wall.

ii) The influence degrees of the oxygen pressure drop on the gas temperatures on the combustor wall are different in the two propellant cases. It is more obvious in the hot propellant case. The gas temperature on the wall is affected mainly by the combustion performance and flow characteristics. The injection velocity in the hot propellant case is relatively fast compared with that in the GH_2/GO_2 case, because of a high initial temperature of the propellants under the condition of the same oxidizer pressure drop ratio. Besides, the combustion performance in the hot propellant case is better, and the temperature of the backflow gas is higher than that in the GH_2/GO_2 case. Therefore, the influence degree in the hot propellant case is remarkable. Since the influence degree of pressure drop ratio on the combustion performance is relatively small compared with that of velocity ratio, the influence on the gas temperature is weak.

iii) There is only little influence of the oxidizer post tip thickness and recess on the combustion performance, so the influence on the gas temperature is slight, too.

iv) In the hot propellant case, the temperature of the backflow gas near the faceplate is affected by the temperature of the hydrogen-rich gas. The high temperature hydrogen-rich gas leads to a high temperature gas near the combustor wall. Yet the oxygen-rich gas is injected near the combustor axis. The combustion surface and the hydrogen-rich gas are located between the oxygen-rich gas and the combustor wall. Its influence on combustion is weak. So the influence of the combustor wall on the gas temperature is weak as well.

Comparing the temperatures on the same injector design parameter and their levels in both propellants cases, it can be seen that the temperature in the hot propellant case is about 800-K larger than that in the GH_2/GO_2 case. It also shows that the heat load of the combustor in the hot propellant case is much larger than that in the GH_2/GO_2 case.

The influence tendencies of the design parameter level on the average value of T_W are shown in Fig. 5. The gas temperature is mainly affected by the combustion performance, and the influence tendencies are almost the same in the two propellant cases, so the tendencies of the temperature are also almost the same.

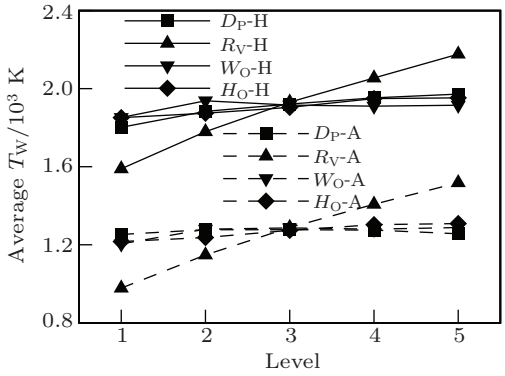


Fig. 5. Effect trends of design parameters on T_W in the hot propellants case and GH2/GO2 case.

3.2.3. Range analysis of T_F

The range analyses on the average gas temperatures on the faceplate for the GH_2/GO_2 case and the hot propellants case are shown in Tables 9 and 10, respectively. In the GH_2/GO_2 case, according to the influence degree, the sequence of the injector parameters from large to small is D_P, R_V, H_O, W_O; while the sequence in the hot propellants case is D_P, R_V, T_H, T_O, H_O, W_O. The reasons are as fellows.

(I) The injection velocity increases with velocity ratio and oxidizer pressure drop ratio increasing, and it has a potential to enhance the backflow near the injector faceplate, thus increasing the gas temperature.

(II) The starting position of the gas–gas combustion is where the propellants start to contact. The recess can move toward the starting position of the combustion. Although it has only a small influence on the combustion performance, it affects the gas temperature of the backflow obviously.

(III) There the injector post tip thickness has only small influence on combustion performance and flow, thus the effect on the gas temperature on the injector faceplate is slight.

(IV) With the same reason as that for the gas temperature on the combustor wall above, the influence of the hydrogen-rich gas temperature is obvious, and that of the oxygen-rich gas temperature is slight.

Comparing the temperatures on the same injector design parameter and their levels in both propellant cases, it can be seen that the temperature in the hot propellant case is about 500-K larger than that in the GH_2/GO_2 case, or say that the temperature is doubled in the hot propellant case. It illustrates that the heat protection of the faceplate in the hot propellants case is relatively difficult.

Table 9. Range analysis results of design parameters on the T_F for the GH_2/GO_2 case.

Parameters	Average of T_F/K					Range
	Level 1	Level 2	Level 3	Level 4	Level 5	
D_P	334.6	402.4	460.2	494.6	535.2	200.6
R_V	368	403.4	441	484	530.6	162.6
W_O	443.4	466.6	451.2	434.8	431	35.6
H_O	409.2	423.6	442.8	466.8	484.6	75.4

Table 10. Range analysis results of design parameters on the T_F for the hot propellants case.

Parameters	Average of T_F /K					Range
	Level 1	Level 2	Level 3	Level 4	Level 5	
D_P	813.4	873.0	946.6	1005.2	1072.4	259.0
R_V	839.0	889.2	926.0	982.4	1074.0	235.0
W_O	936.2	987.8	954.8	907.4	924.4	80.4
H_O	904.2	910.4	910.4	971.2	988.4	84.2
T_O	907.8	898.2	951.6	989.0	964.0	90.8
T_H	873.4	905.6	949.0	986.8	995.8	122.4

The influence tendencies of the injector parameters on the average gas temperature on the faceplate are shown in Fig. 6. It can be seen that the temperature increases with the level of the design parameter increasing, except for thickness of the oxidizer post tip. As its thickness increases, the temperature increases at the beginning, and then it will decrease. The major factor for the gas temperature on the faceplate is the temperature of the backflow gas. As the thickness increases, the combustion performance improves a little. However, the size of the injector becomes larger, so that the backflow region diminishes. When the thickness is small, the main factor is the combustion performance, thus the temperature near the faceplate increases. And when the thickness is large, the main factor becomes the backflow region. A small region can weaken the backflow, thus reducing the temperature. Comparing the two propellant cases, the influence tendencies for the parameters are also almost the same.

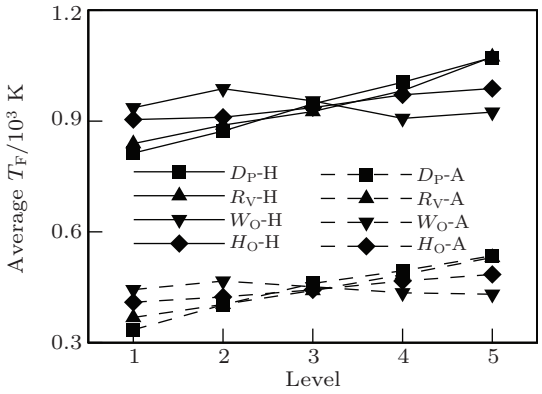


Fig. 6. Effect trendd of design parameters on T_W in the hot propellant case and GH_2/GO_2 case.

3.3. Experimental validation

3.3.1. Parameters of injectors

The objective of the experiments is to validate the simulation results. However, if the experiments are carried out according to the simulation cases, 50 injectors need to be fabricated, which will be very time consuming, and lead to a large cost. To solve those issues, the method of single factor analysis is applied in the study.

In the simulation results, the influences of the velocity ratio on the combustion performance and the heat load of the combustor, and the pressure drop ratio on the heat load are remarkable. The influences of other parameters are relatively weak. Therefore, the velocity ratio and the oxidizer pressure drop ratio are selected. The experiments are divided into two groups to investigate the two parameters respectively. The values of the injector design parameters are shown in Table 11. Both GH_2/GO_2 and hot hydrogen-rich gas/oxygen-rich gases are used as the propellants. The mass flow rate and the temperature of the GH_2/GO_2 are the same in the simulation. The parameters of the hot propellants are shown in Table 12.

Table 11. Values of injector design parameters.

Group	D_P/%	R_V	W_O/mm	H_O/mm
1	2.5, 4.0, 6.5, 10, 15	6.6	1.5	0
2	6.5	3, 4, 6.6, 9	1.5	0

Table 12. Values of injector design parameters.

Group	T_O	T_H	$\dot{m}_O$/mm	$\dot{m}_H$/mm
1	295	295	193.7	32.3
2	676	758	180	46

3.3.2. Experimental facilities

The diameter and the length of the combustor for the experiments are the same as those for the simulation. The hydrogen-rich gas and the oxygen-rich gas are provided by the GH_2/GO_2 hydrogen-rich and the GH_2/GO_2 oxygen-rich preburners, respectively. The detailed experimental system and the approach can be seen in Ref. [26].

The combustor consists of two parts: the inner sleeve and the outer sleeve, which can be seen in Fig. 7. The temperature sensors are fixed on the outer sleeve at the tip of each sensor where it contacts the outer wall of the inner sleeve. The outer wall temperatures of the inner sleeve along the combustor axial direction are measured in the experiments to evaluate the heat load of the combustor. The distance between the contacting point of the sensors and the inner wall of the combustor is 13 mm. The starting fixed position of the sensor is 28 mm away from the injector, and the interval between sensors is 15 mm. The number of installed sensors is 15.

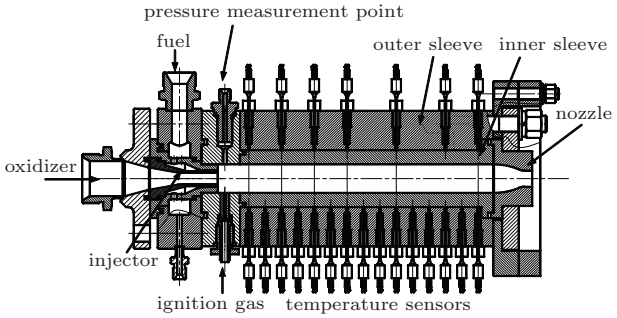


Fig. 7. Schematic plot of the combustor.

The characteristic velocity efficiency is selected as the indicator of the combustion performance, and is given by

$$\eta = \frac{p_C A_t}{\dot{m}_C} / C^*,$$

where p_C is the experimental pressure of the combustor, A_t represents the throat area, and C^* denotes the theoretical characteristic velocity efficiency.

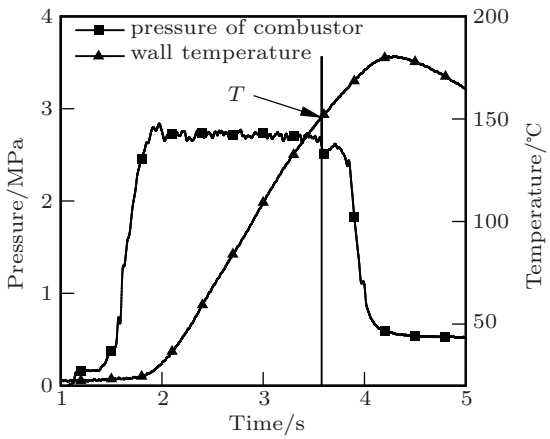


Fig. 8. Typical pressure in the experiment.

The typical experimental results are shown in Fig. 8. The test lasts for 2 s. Approximately 0.3 s after starting up, the combustor pressure becomes stable, which means that it can be used to calculate the characteristic velocity efficiency. For the heat transfer from the inner sleeve, the temperature still rises after shutting down. As a result, the temperature after the experiment shutting down is selected as the wall temperature.

3.3.3. Experimental results and analysis

The influence of the oxidizer pressure drop ratio on the wall temperature is shown in Fig. 9. It can be seen that the wall temperatures increase with oxidizer pressure drop ratio increasing in both propellant cases, which is more obvious in the hot propellant case. The wall temperatures in the hot propellant case are higher than that in the GH_2/GO_2 case at the same oxidizer pressure drop ratio, and it is almost doubled in the forepart of the combustor. A high temperature and a fast injection velocity of the hot propellant enhance the heat transfer. Furthermore, the high momentum ratio is another reason for the combustion performing very well. In the simulations, as the oxidizer pressure drop ratio increases, the gas temperatures increase in both propellants cases as well. The influence degree in the hot propellant case is larger than that in the GH_2/GO_2 case. The gas temperature in the hot propellant case is larger than that in the GH_2/GO_2 case. Although the gas temperature in simulations is different from the wall temperatures in experiments, the wall temperatures are influenced by the gas temperature on the combustor wall. Besides, they have the same tendency in the two propellant cases in the sense of the oxidizer pressure drop ratio. Therefore, the simulation results are validated through an indirect way of using the experimental wall temperatures. Due to the combustion completion, the differences between wall temperatures in different oxidizer pressure drop ratio conditions diminish in the rear part of the combustor. The simulation and experimental results all show that the heat load of the combustor in the hot propellant case is larger than that in the GH_2/GO_2 case. However, for the heat transfer of the propellant temperature on the forepart of the combustor, how to use the results from the GH_2/GO_2 case to analyze the hot propellants case needs in-depth study.

The characteristic velocity ratios for different oxidizer pressure drop ratios and propellants are shown in Fig. 10. They all decrease with the oxidizer pressure drop ratio increasing. The increase of the heat loss is one of the reasons for a large pressure drop. The combustion length becomes longer when the oxidizer pressure keeps increasing. However, the combustion can be completed in the combustor in the simulations. Therefore, it cannot be validated directly that the combustion length is affected by the oxidizer pressure drop ratio. The higher the oxidizer pressure drop ratio, the larger heat load and the lower efficiency can be yielded, which also provides some information for the injector design.

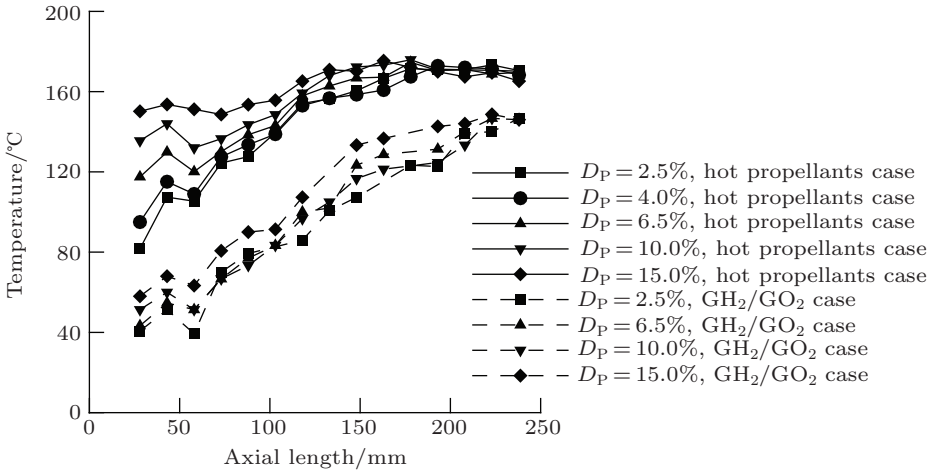


Fig. 9. Wall temperatures in different velocity ratio cases.

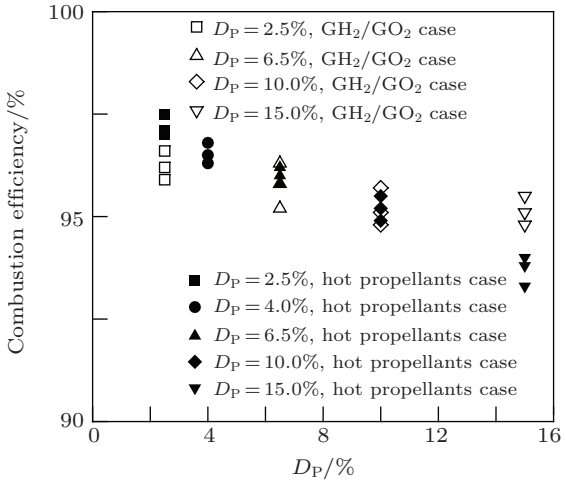


Fig. 10. Characteristic velocity efficiencies in different pressure drop cases.

The influences of the velocity ratio on wall temperature are shown in Fig. 11. The wall temperatures increase as the velocity ratio increases in both propellants cases. The wall temperatures are relatively large in the hot propellant case. From the above simulation results of the velocity ratio it follows that the influence tendency of the velocity ratio on the wall temperature in experiment is almost the same as that on the gas temperature of the combustor wall in simulation. It can be seen that the influence of the velocity ratio on the wall temperature in the GH_2/GO_2 case is obviously higher than that in the hot propellant case. In the GH_2/GO_2 case, the propellant is at an ambient temperature. If the gas temperature near the combustor wall does not change a lot, the wall temperatures cannot increase remarkably even when the velocity increases, which means that the gas temperature in the experiment increases and the combustion performance is improved with velocity ratio increasing. The simulation results which prove the combustion performance can be improved by increasing the velocity ratio are validated by experiments. Compared with the variation of oxidizer pressure drop ratio, the change of the wall temperature that is caused by the velocity ratio is very obvious. The order of the influence degree in the experiments is the same as that in the simulations. However, in the hot propellant case the initial temperature of the propellant is relatively high, and the improvement on the combustion performance at the gas temperature on the wall is weakened. Therefore, the influence degree is relatively weak.

The characteristic velocity efficiencies are shown in Fig. 12. In the GH_2/GO_2 case, the efficiency is very low when the velocity ratio is 3, and the wall temperatures are low as well, which implies that the combustion is inadequate. In other words, a low velocity is not beneficial to improving the mixing and the combustion. The efficiency becomes relatively high when the velocity ratio exceeds 4. However, the more the heat loss in the larger velocity ratio case, the lower the efficiency will be. In the hot propellant case, the efficiency can be largest when the velocity ratio is 3. It illustrates that the combustion performs very well in the hot propellants. The combustion length in the hot propellant case is about 50 mm less than that in the GH_2/GO_2 case in the simulation results. Therefore, even though the combustion cannot be completed in the GH_2/GO_2 case, it is likely to be completed in the hot propellant case. It can be validated by the results of the case where the velocity ratio is 3. For the same reason in the GH_2/GO_2 case, the efficiency is reduced as the velocity ratio increases in the hot propellant case.

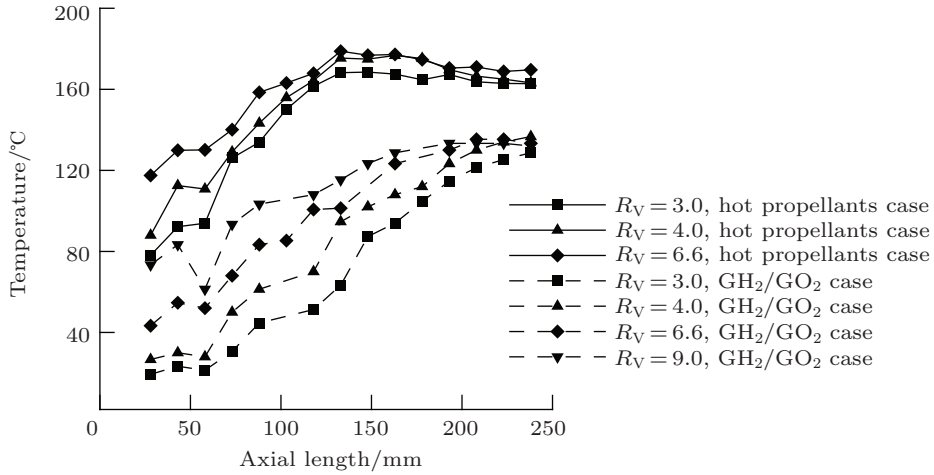


Fig. 11. Wall temperatures in the different velocity ratio cases.

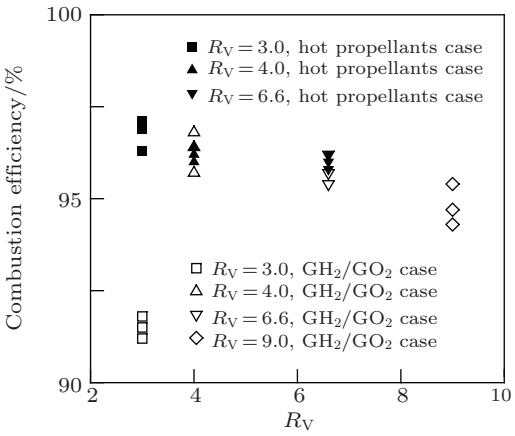


Fig. 12. Characteristic velocity efficiencies in different velocity ratio cases.

4. Conclusion

With the different propellants, the simulation results obtained by the orthogonal experimental design method show that the influence tendencies of the injector parameters on combustion length, average gas temperatures on the combustor wall, and the faceplate are similar. The shearing effect is the main influencing factor on the combustion performance in the shear coaxial injector. Under the same conditions of the velocity ratio and the oxidizer pressure drop, the shearing effect between the fuel and the oxidizer changes little, so the combustion performances are almost the same in different temperature cases.

The simulation results are consistent with experimental values, illustrating that the trends of R_V and D_P influence on the combustion length and the heat load of the combustion in both cases are similar. That is larger R_V yields shorter combustion length and larger heat load of combustor. As D_P increases, the combustion length increases. With the same R_V, the fuel injection velocity is positively correlated with D_P, therefore, the recirculation near the injector face is enhanced and heat load is larger. For a shear coaxial injector, it is feasible to predict the regularity and the trend in the hot propellant case by using the results in the ambient temperature propellant case.

The numerical and experimental quantitative results show that the better combustion is conducted to obtain better performances but also larger heat load in the hot case. With the same injector parameters in both cases, the ratio of momentum, the size of injector, and the area of shear mixture, which can enhance the combustion velocity and improve the performance, are larger in the hot ones, making the combustion length about 50 mm shorter than that in the GH_2/GO_2 case.

For a shear coaxial injector, it is feasible to predict the regularity and the trend in the hot propellant case by using the results in the ambient temperature propellant case, but more complex work has to be done for the quantitative research of combustion performance and thermal protection in the hot gas case.

References

[1] Hunter U and Hutt J J 2003 12*th AIAA International Space Planes and Hypersonic Systems and Technologies,* December 15–19, 2003, Norfolk, Virginia, USA, AIAA-2003-6941

[2] Davis J A and Campbell R L 1997 33*rd AIAA/ASME/SAE/ASEE Joint Propulsion Conference and Exhibit*, July 6–9, 1997, Seattle, WA, USA, AIAA-1997-3318

[3] Tucker P K, Klem M D, Smith T D, Farhangi S, Fisher S C and Santoro R J 1997 33*rd AIAA/ASME/SAE/ASEE Joint Propulsion Conference and Exhibit,* July 6–9, 1997, Seattle, WA, USA, AIAA-1997-3350

[4] Farhangi S, Yu T, Rojas L and Sprouse K 1999 35*th AIAA/ASME/SAE/ASEE Joint Propulsion Conference and Exhibit,* June 20–24, 1999, Los Angeles, CA, USA, AIAA-1999-2757

[5] Vaidyanathan A, Gustavsson J and Segal C 2010 *Journal of Propulsion and Power* **26** 186

[6] Cai G B, Wang X W, Jin P, Du Z G and Gao Y S 2008 44*th AIAA/ASME/SAE/ASEE Joint Propulsion Conference and Exhibit,* July 21–23, 2008, Hartford, CT, USA, AIAA-2008-4562

[7] Wang X W, Cai G B, Gao Y S and Jin P 2009 45*th AIAA/ASME/SAE/ASEE Joint Propulsion Conference and Exhibit,* August 2–5, 2009, Denver, Colorado, USA, AIAA-2009-5042
[8] Tramecourt N, Masquelet M and Menon S 2005 41*st AIAA/ASME/SAE/ASEE Joint Propulsion Conference and Exhibit,* July 10–13, 2005, Tucson, Arizona, USA, AIAA-2005-4124
[9] Schley C A, Hagemann G, Tucker P K, Venkateswaran S and Merkle C L 1997 33*rd AIAA/ ASME/SAE/ASEE Joint Propulsion Conference and Exhibit,* July 6–9, 1997, Seattle, WA, USA, AIAA-1997-3302
[10] Foust M J, Deshpande M, Pal S, Ni T, Merkle C L and Santoro R J 1996 34*th Aerospace Sciences Meeting and Exhibit,* January 15–18, 1996, Reno, NV, USA, AIAA-1996-0646
[11] Coy E B 2008 26*th AIAA Aerodynamic Measurement Technology and Ground Testing Conference,* June 23–26, 2008 Seattle, Washington, USA, AIAA 2008-3952
[12] Locke J M, Pal S, Woodward R D and Santoro R J 2009 45*th AIAA/ASME/SAE/ASEE Joint Propulsion Conference and Exhibit,* August 2–5, 2009, Denver, Colorado, USA, AIAA-2009-5395
[13] Shyy W, Tucker P K and Vaidyanathan R 2001 *Journal of Propulsion and Power* **17** 391
[14] Vaidyanathan R, Tucker P K, Papila N and Shyy W 2004 *Journal of Propulsion and Power* **20** 705
[15] Conley A, Vaidyanathan A and Segal C 2007 *Journal of Spacecraft and Rockets* **44** 633
[16] Marshall W M, Pal S, Woodward R D and Santoro R J 2005 41*st AIAA/ASME/SAE/ASEE Joint Propulsion Conference and Exhibit,* July 10–13, 2005, Tucson, Arizona, USA, AIAA-2005-3572
[17] Lin J, West J, Williams R W and Tucker P K 2005 41*st AIAA/ASME/SAE/ASEE Joint Propulsion Conference and Exhibit,* July 10–13, 2005, Tucson, Arizona, USA, AIAA-2005-4524
[18] Tucker P K, Menon S, Merkle C L, Oefelein J C and Yang V 2008 44*th AIAA/ASME/SAE/ASEE Joint Propulsion Conference and Exhibit,* July 21–23, 2008, Hartford, CT, USA, AIAA-2008-5226
[19] Sozer E, Vaidyanathan A, Segal C and Shyy W 2009 47*th AIAA Aerospace Sciences Meeting Including The New Horizons Forum and Aerospace Exposition*, January 5–8, 2009, Orlando, Florida, USA, AIAA-2009-0449
[20] Betti B, Martelli E and Nasuti F 2010 46*th AIAA/ASME/SAE/ASEE Joint Propulsion Conference and Exhibit,* July 25–28, 2010, Nashville, TN, USA, AIAA-2010-6721
[21] Wang W, Jin P and Cai G 2009 *Journal of Beijing University of Aeronautics and Astronautics* **35** 1095 (in Chinese)
[22] Wang X W, Cai G B and Jin P 2010 *Chin. Phys. B* **19** 019401
[23] Wang X W, Cai G B and Jin P 2011 *Chin. Phys. B* **20** 104701
[24] Wang X W, Cai G B and Jin P 2011 *Chin. Phys. B* **20** 064701
[25] Gao Y S, Li M W, Wang X, Jin P, Yu N and Cai G B 2011 62*nd International Astronautical Congress*, October 1–5, 2011, Cape Town, South Africa, IAC-11.C4.3.10
[26] Li M, Gao Y S, Jin P, Yu N J, Ma B and Cai G B 2010 *Journal of Propulsion Technology* **31** 696 (in Chinese)